

Distortion Reduction in Moving-Coil Loudspeaker Systems Using Current-Drive Technology*

P. G. L. MILLS** AND M. O. J. HAWKSFORD

University of Essex, Wivenhoe Park, Colchester, Essex, CO4 3SQ, UK

The performance advantages of current-driving moving-coil loudspeakers is considered, thus avoiding thermal errors caused by voice-coil heating, nonlinear electromagnetic damping due to $(Bl)^2$ variations, and high-frequency distortion from coil inductive effects, together with reduced interconnect errors. In exploring methods for maintaining system damping, motional feedback is seen as optimal for low-frequency applications, while other methods are considered. The case for current drive is backed by nonlinear computer simulations, measurements, and theoretical discussion. In addition, novel power amplifier topologies for current drive are discussed, along with methods of drive-unit thermal protection.

0 INTRODUCTION

The moving-coil drive unit is by far the most widely used electroacoustic transducer in both high-performance studio and domestic audio installations, as well as in general-purpose sound reinforcement. Consequently it has attracted numerous studies to investigate its inherent distortion mechanisms (see, for example, [1]–[11]), which as a consequence are well understood. Much work has also been carried out on improving drive-unit linearity by the application of motional feedback techniques, which provide a useful enhancement in performance at low frequencies. Improvements to the basic regime of motional feedback have been made by including an additional current feedback loop [12], [13], which is reported to reduce high-frequency distortion. This method is a specific implementation of what we will term *current drive*, a subject that, it is felt, has not received the attention it deserves.

This paper therefore aims to explore in detail the benefits of current drive in reducing the dependence of drive-unit performance on motor system nonlinearities, in particular the voice-coil resistance which undergoes significant thermal modulation.

In a conventional voltage-driven system (one where the power amplifier output voltage is regarded as the

information-representing quantity), the current is initially limited by the series elements of voice-coil resistance and inductance, together with the interconnect and amplifier output impedance. A force related to the current in the system then acts on the drive unit moving elements as a result of the motor principle, and once motion occurs, an electromotive force is induced in the coil to oppose the applied signal voltage, thus constraining the magnitude of current flow. The accuracy to which the drive-unit velocity responds to the applied signal is, therefore, dependent on the series elements in the circuit, and any signal-related changes in their value will result in distortion.

The voice-coil resistance is of specific concern, as it is usually a dominant element. As a result of self-heating in excess of 200°C, a significant increase in coil resistance occurs of typically 0.4%/°C for copper, leading to sensitivity loss, lack of damping, and crossover misalignment. In their paper, Hsu et al. [6] concluded that a satisfactory method of compensating for this effect had yet to be found.

At higher audio frequencies, the coil inductance also becomes significant, resulting in a loss of sensitivity. In addition, the inductance suffers dynamic changes with displacement, providing a distortion mechanism which is further complicated by eddy current coupling to the pole pieces in the magnetic circuit [14, pt. 1]. A further problem is distortion mechanisms at the amplifier–loudspeaker interface, such as interconnect errors [14, pt. 4] and interface intermodulation distortion

* Manuscript received 1988 February 17.

** Now at Tannoy Ltd., Rosehall Industrial Estate, Coatbridge, Strathclyde, ML5 4TF, UK.

[15]–[17].

To overcome these limitations, the drive unit should be current rather than voltage controlled and interfaced directly to a power amplifier configured as a current source, thus offering a high output impedance. The performance advantages of this technique are discussed in detail, supported by computer simulation of the non-linear system together with objective measurement on a prototype two-way active loudspeaker system.

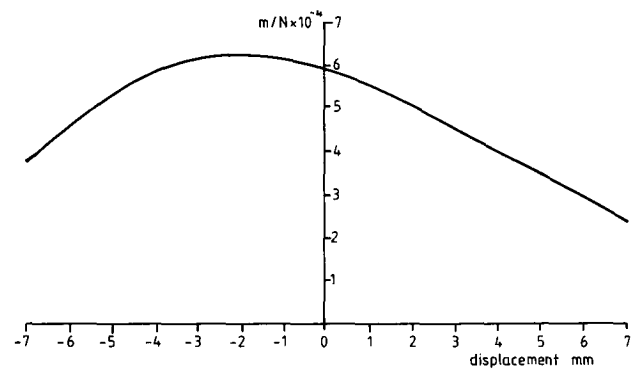
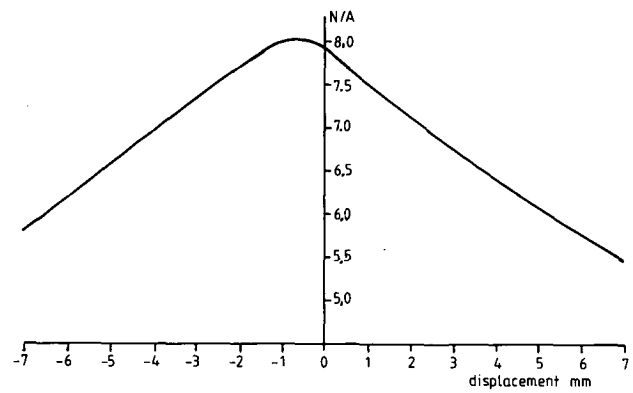
To complement this study, the application of both motional feedback and noninteractive frequency response shaping as a means of aligning the drive unit Q to the required value is discussed. Finally, the topic of current source power amplifier design is considered along with the presentation of some novel types of circuit topology, while the subject of drive-unit protection under current drive is also examined.

The technique of current drive in active loudspeaker systems is seen as being of particular importance in view of the performance advantages demonstrated over conventional systems in terms of both reduced linear and nonlinear distortion. For high-quality system design, current drive is seen as the more logical methodology, with voltage drive appearing as the result of established practice and convenience.

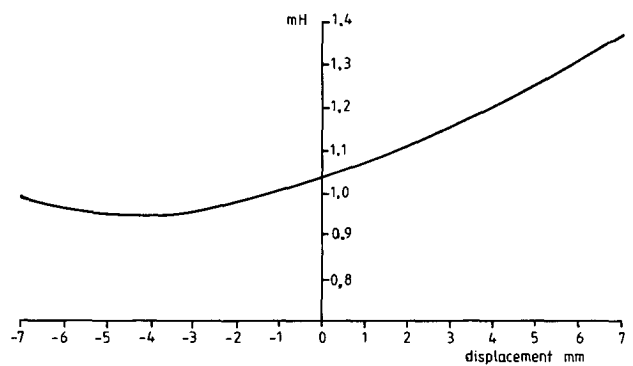
1 LOUDSPEAKER PERFORMANCE UNDER VOLTAGE DRIVE

In order to establish a performance reference, this section considers motor system linearity for a moving-coil drive unit under conventional voltage drive. For the tests, a Celestion SL600 135-mm-diameter bass-midrange driver was used, mounted in its enclosure. It was chosen partly due to the excellent cone and surround behavior, meaning that the distortion contribution of these elements is small.

To enable performance predictions under general signal excitation to be made, the variation of parameters with coil displacement was measured. This is shown in graphic form, in Fig. 1 for Bl product, compliance, and coil inductance. The linear parameters for the model are given in Table 1, which explains the terminology and also the equivalence between the electrical model and the mechanical model used. The approach broadly



(b)



(c)

Fig. 1. Variation of model parameters with displacement. Negative displacement indicates motion toward magnet. (a) Bl product. (b) Mechanical compliance. (c) Electric coil inductance.

Table 1. Model parameters for example drive unit.

Parameter	Electrical model	Mechanical model
Voice-coil resistance	$R_e = 7.0 \Omega$	$R_{me} = (Bl)^2/R_e$ kg/s
Voice-coil inductance	L_e^*	$C_{me} = L_e/(Bl)^2$ m/N
Enclosure compliance	$L_{cmb} = C_{mb}(Bl)^2$	$C_{mb} = 750 \times 10^{-6}$ m/N
Suspension compliance	$L_{cms} = C_{ms}(Bl)^2$	C_{ms}^* m/N
Moving mass	$C_{mes} = M_{ms}/(Bl)^2$	$M_{ms} = 0.0183$ kg
Mechanical resistive losses	$R_{es} = (Bl)^2/R_{ms}$	$R_{ms} = 2.4336$ kg/s
Source impedance	Z_g (assume zero)	$Z_{mg} = (Bl)^2/Z_g$ kg/s

Bl = force factor (N/A)*

* Indicates nonlinear elements.

follows that of Small [18], except that a mechanical model is used in preference to the acoustic one. Fig. 2(a) shows the equivalent electrical model for the drive unit, connected to an amplifier and interconnect of series source impedance Z_g , showing the mechanical impedance as a lumped quantity Z_m . Analysis of this model gives the transfer function between amplifier output voltage and cone velocity,

$$u = \frac{V_0 Bl}{Z_m [Z_s + (Bl)^2/Z_m]} \quad (1)$$

where

- u = cone velocity, meters per second
- V_0 = amplifier source voltage, volts
- B = flux density for motor system, tesla
- l = coil length in field B , meters
- Z_m = lumped mechanical impedance, kilograms per second
- Z_s = lumped electric impedance (Z_g , R_e , and sL_e), ohms.

Referring the mechanical impedance to the "primary" of the Bl transformer to show its constituents gives the electrical model of Fig. 2(b), while referring the electrical parameters to the "secondary" results in the mechanical model of Fig. 2(c). Both these models are useful in the forthcoming discussion, although emphasis is placed on the mechanical system.

The mechanical model forms the basis of a transient analysis procedure, which can readily incorporate nonlinear parametric variations. The details of this approach

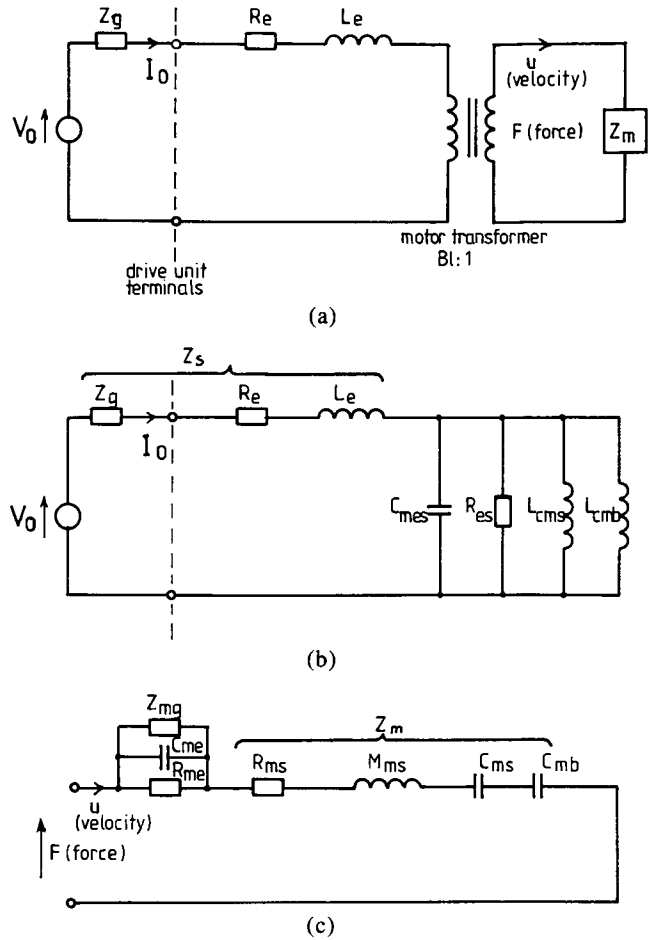


Fig. 2. Modeling of drive unit in sealed enclosure, under voltage drive. (a) Basic electromechanical model. (b) Electrical model. (c) Mechanical model.

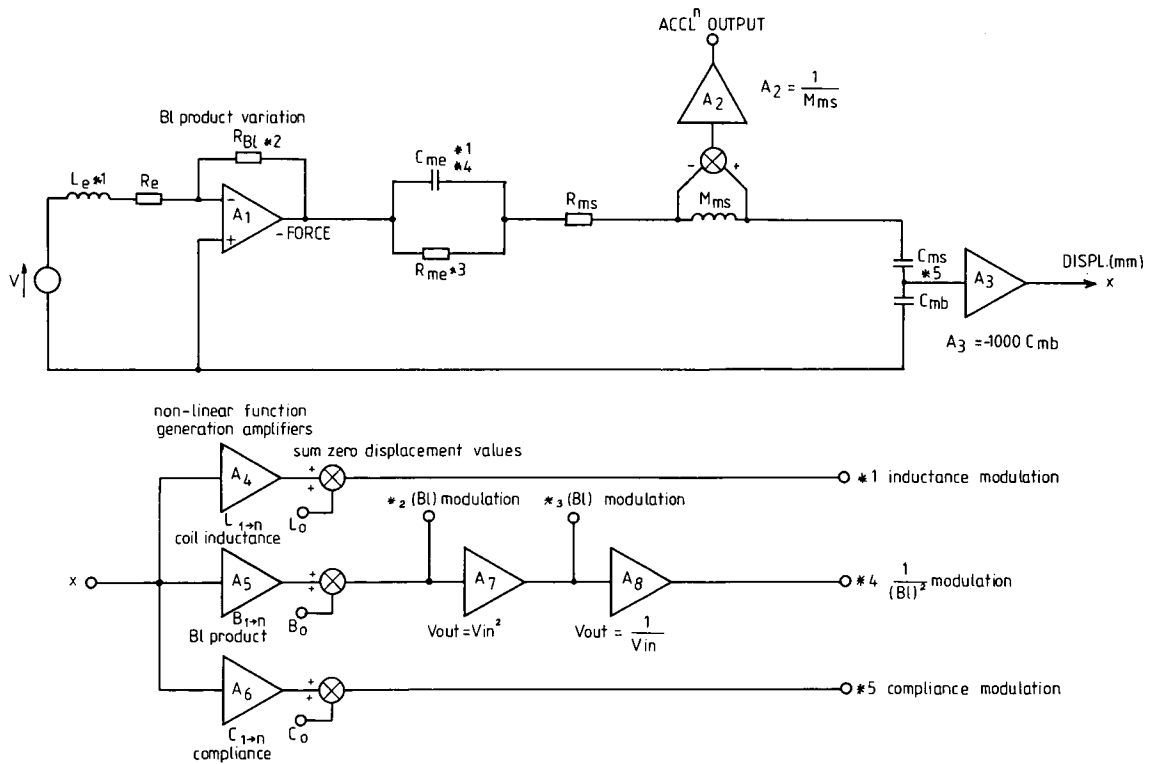


Fig. 3. Simplified nonlinear model for voltage-driven simulation.

were given in an earlier paper [19], where it was seen to avoid the approximations forced by an analytical solution. It may be contrasted to that of Kaizer [3], where drive-unit nonlinearity was modeled by Volterra series expansion. Fig. 3 shows the simplified circuit for the computer model, where it is assumed that the driving amplifier has zero source impedance. The output quantity acceleration is derived from the voltage across the moving mass element M_{ms} , while a signal proportional to displacement is obtained from the voltage across the enclosure compliance C_{mb} . This displacement voltage is used to drive three nonlinear amplifiers A_4 , A_5 , and A_6 , whose transfer characteristics are expressed as polynomials, representing the measured variation in coil inductance, Bl product, and compliance, respectively. A technique was adopted whereby the three nonlinear functions were first represented by a Fourier series from which the corresponding polynomials were generated. A 30th-order approximation to each function was deemed necessary to avoid undue error. The zero displacement values for these parameters were then summed by constant factors L_0 , B_0 , and C_0 . Each of the modulation outputs in the diagram is coded by an asterisk and number to indicate which circuit parameters it modulates.

To produce distortion predictions from this model, a sine wave input is used and the system allowed to reach steady state. A single cycle is then sampled as input data to a fast Fourier transform, which indicates the relative amplitude of the distortion harmonics.

At 100 Hz, with the source voltage chosen to give a current of 1 A peak, a reasonable relation between theoretical and measured distortion spectra can be seen

in Fig. 4. The model slightly overestimates most distortion components, probably due to errors in measuring the nonlinear parameters. However, at high frequency the model does not prove usable, due to factors such as the complicated nature of eddy current losses and hysteresis effects in the magnetic circuit. The measured 3-kHz at 1A peak distortion spectra are shown in Fig. 5, while intermodulation products between 50-Hz and 1-kHz sine wave inputs of equal amplitude are shown in Fig. 6.

The effect of voice-coil heating is a major problem under voltage drive, and it is interesting to note the severe difficulty in obtaining these measurements due to the sensitivity loss and frequency response errors which occur as the coil heats up. A further problem caused by heating is that of crossover misalignment in the case of passive systems. To illustrate this effect, Fig. 7 shows an idealized two-way second-order crossover aligned to 3.4 kHz. The drive units are represented by resistive elements, and the overall system transfer function is evaluated by effectively subtracting the high-pass and low-pass outputs. Fig. 8 then compares the system transfer function arising from coil heating to 200°C with the intended response at 20°C. Although oversimplistic, this model does show that large errors can result.

Errors due to interconnect effects are also seen to be of importance. Measurements of the error across a selection of 5-m interconnects have revealed errors up to 15 dB below the main signal. It is worth noting that the error is a function of drive-unit-crossover impedance and, while mainly linear, also contains a nonlinear component due to the nonlinear nature of the load.

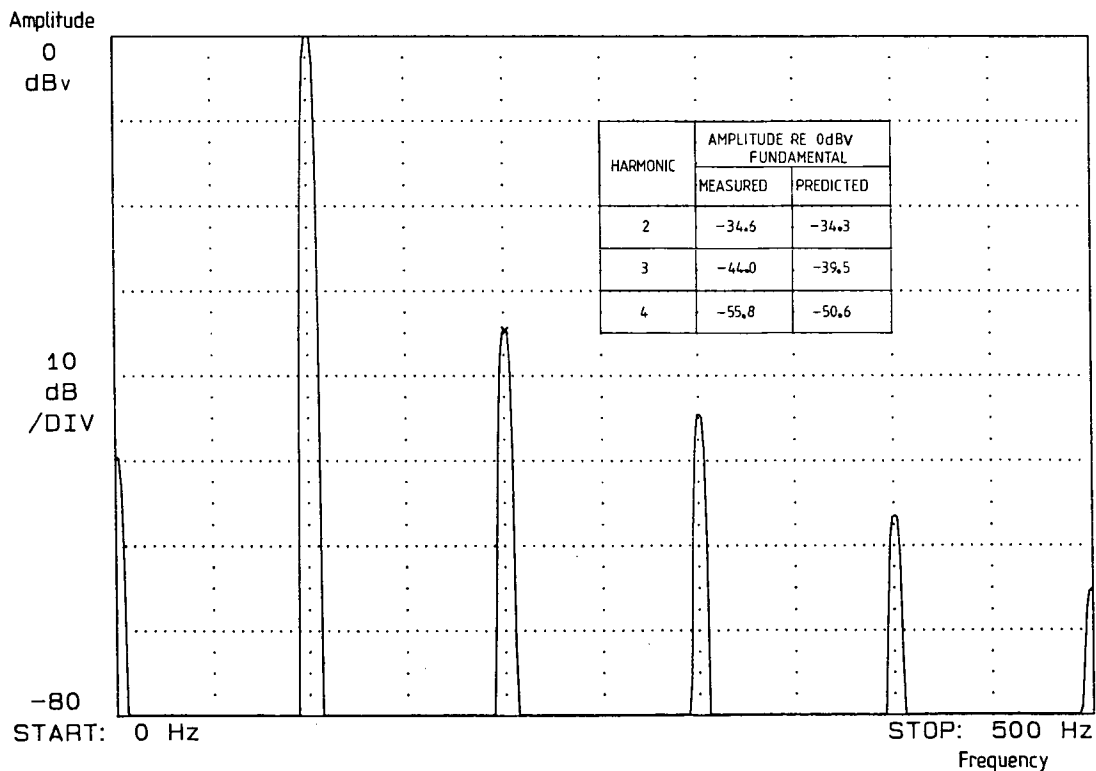


Fig. 4. Measured 100-Hz harmonic distortion, voltage driven. Table compares with predicted result.

2 THE CASE FOR CURRENT DRIVE

To assess the performance advantages of a current-driven moving-coil drive unit, a similar procedure is adopted to that of Sec. 1, though a current source is substituted for the voltage source, with output impedance assumed infinite. An immediate consequence of

this strategy is that the series elements of coil resistance, coil inductance (with attendant eddy current losses), and interconnect lumped series elements, together with Bl and the lumped mechanical impedance no longer influence the instantaneous driving current. The significance of this observation is best illustrated by examining the current-driven velocity transfer function,

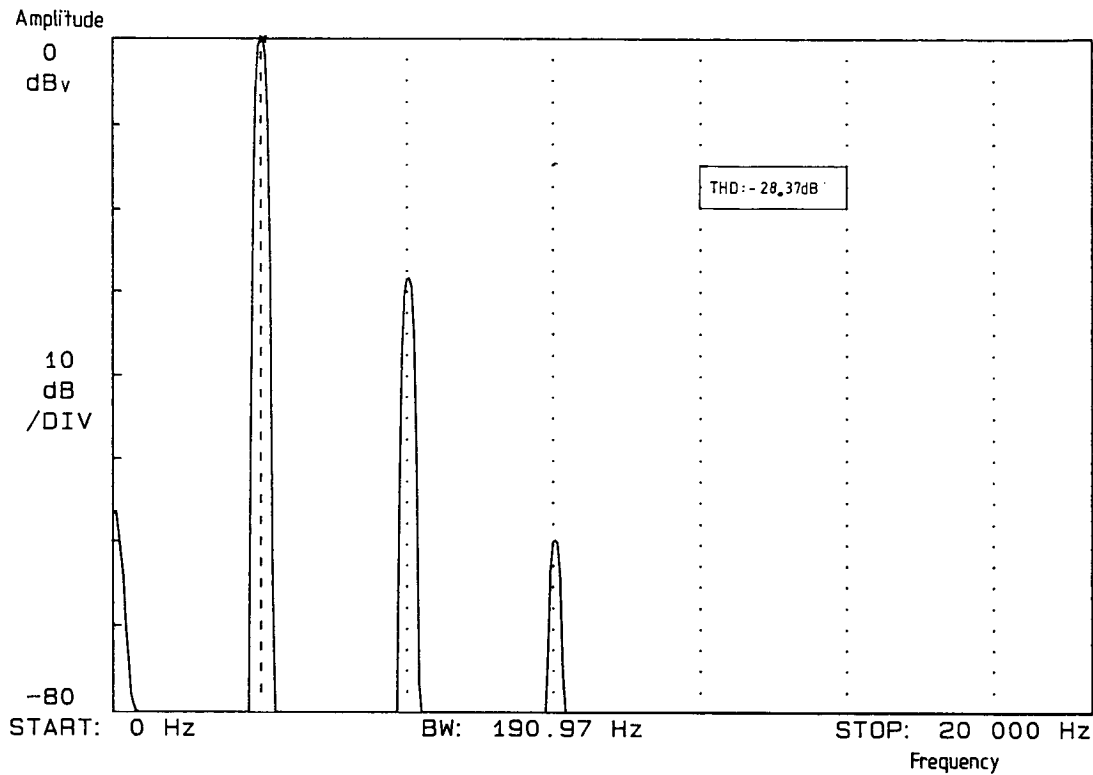


Fig. 5. Measured 3-kHz harmonic distortion, voltage driven.

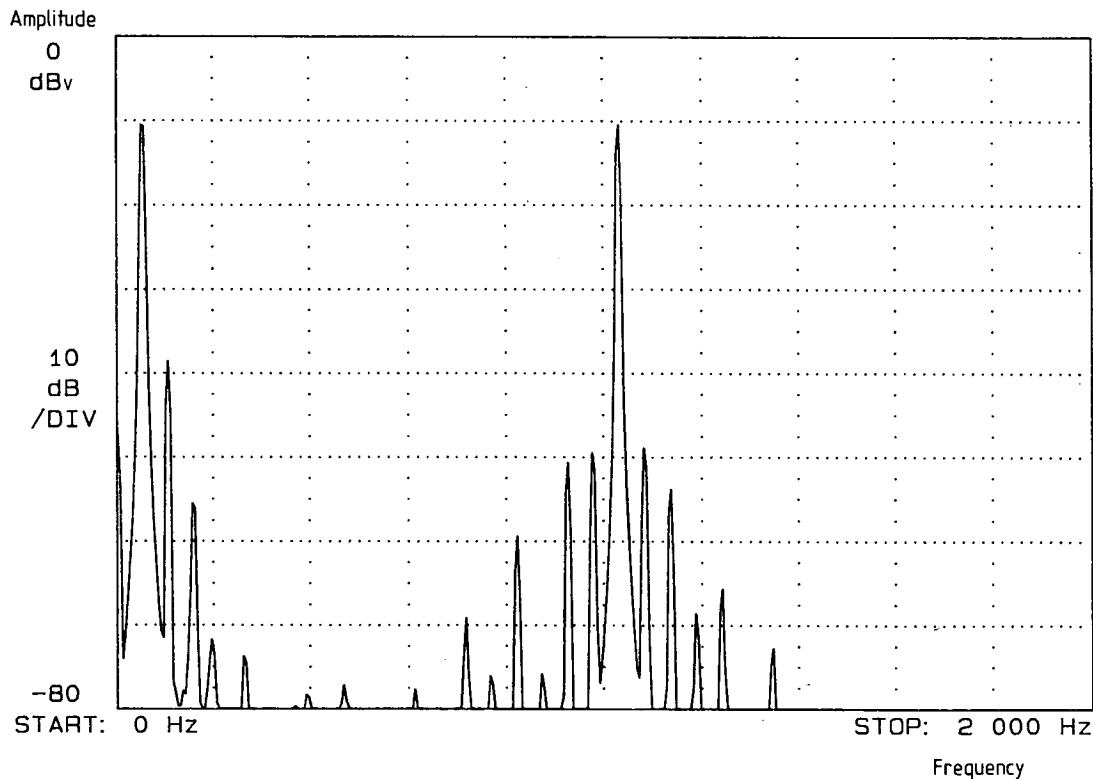


Fig. 6. Measured 50-Hz and 1-kHz intermodulation distortion, voltage driven.

$$u = \frac{I_0 B l}{Z_m} \tag{2}$$

where I_0 is the amplifier output current in amperes.

Comparison with the voltage-driven case, Eq. (1), shows that for current drive, the transfer function is of a simpler form, independent of the terms Z_s and $(Bl)^2$. It is therefore anticipated that lower distortion will result from elimination of the term $[Z_s + (Bl)^2/Z_m]$. Performance is therefore free of any linear and nonlinear contributions from Z_s , the $(Bl)^2$ term, and shows a reduced dependence on compliance nonlinearity within Z_m , together with any frequency-dependent nonlinear interactions. The mechanical model for the drive unit and enclosure is then reduced to that of Fig. 9.

To demonstrate this claim, a transient analysis at 100 Hz with 1-A peak drive current was performed, using the nonlinear model of Fig. 10. A reasonable match between measured and predicted distortion is again obtained, as shown by Fig. 11.

Comparing this result with the voltage-driven case (Fig. 4) shows a measured and predicted distortion reduction of around 9 dB for the second harmonic, with third- and fourth-order products being reduced by between 3 and 7 dB, depending on whether the measured or the predicted values are taken (the predicted results yielding the better distortion reduction).

Regarding the 3-kHz at 1A peak measurement given in Fig. 12, this shows a substantial reduction of over 26 dB to the voltage-driven result in Fig. 5. Likewise, the 50-Hz–1-kHz intermodulation distortion is improved, as indicated by Fig. 13.

These results show the importance of eliminating the distortion contributions of the $(Bl)^2$ and Z_s terms in a relative comparison between current drive and voltage drive. Thus at the high-frequency end of the drive unit's operating range, the elimination of performance dependence on coil inductance modulation and eddy current losses is seen to be a valuable asset. Further, the current-driven system is completely free from any voice-coil thermal effects. Although the argument is based on a bass–midrange drive unit, with significant cone displacement, tweeters were found to

benefit also, with a more modest 3–7-dB measured distortion reduction across the band, along with the elimination of coil-heating effects.

Finally, the performance independence on linear interconnect errors is also welcome when a low shunt capacitance cable is chosen—a high resultant series inductance being of no significant consequence.

3 DRIVE-UNIT TRANSFER FUNCTION ALIGNMENT UNDER CURRENT DRIVE

Small signal analysis reveals that under current drive, there is a change in frequency response compared with the voltage-driven case, the principal cause being the loss in electromagnetic damping from the low-impedance voice-coil circuit. Consequently, the drive unit Q at fundamental resonance rises to that determined by the mechanical parameters—generally too high for optimal system alignment. To illustrate this, Fig. 14 compares the measured frequency responses of our example drive unit under both current drive and voltage drive. The rise in output around the fundamental resonance under current drive should be noted, along with a reduction in high-frequency rolloff due to the voice-coil inductance no longer appearing in the system transfer function.

In order to realign the acoustic transfer function, three methods have been investigated.

3.1 Electronic Equalization Using Open-Loop Compensation

The addition of a low-level equalizer to redefine the low-frequency alignment of a drive unit under voltage drive is a well-documented technique [20], [21]. The approach is equally applicable to current drive. If the drive-unit transfer function is of the form

$$G(s) = \frac{s^2 T_s^2}{s^2 T_s^2 + s T_s / Q_m + 1}$$

where T_s is the time constant of fundamental resonance, in seconds, and Q_m is the mechanical drive-unit Q , and the desired low-frequency target alignment is written

$$G_t = \frac{s^2 T_c^2}{s^2 T_c^2 + s T_c / Q_c + 1}$$

where T_c is the redefined system time constant, in seconds, and Q_c is the compensated Q value, then, assuming a second-order low-frequency alignment is retained, the equalizer transfer function is defined:

$$X(s) = \left(\frac{s^2 T_c^2}{s^2 T_c^2 + s T_c / Q_c + 1} \right) \times \left(\frac{s^2 T_s^2 + s T_s / Q_m + 1}{s^2 T_s^2} \right)$$

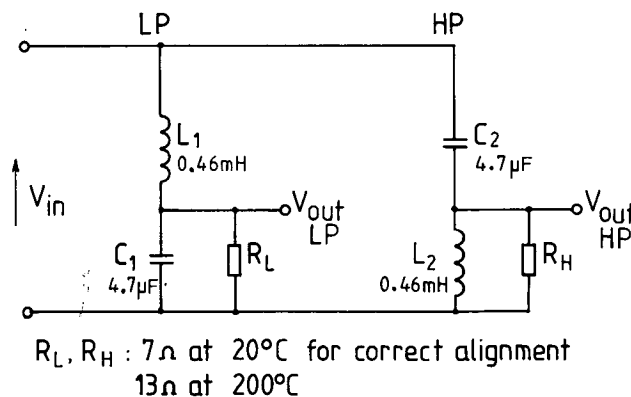
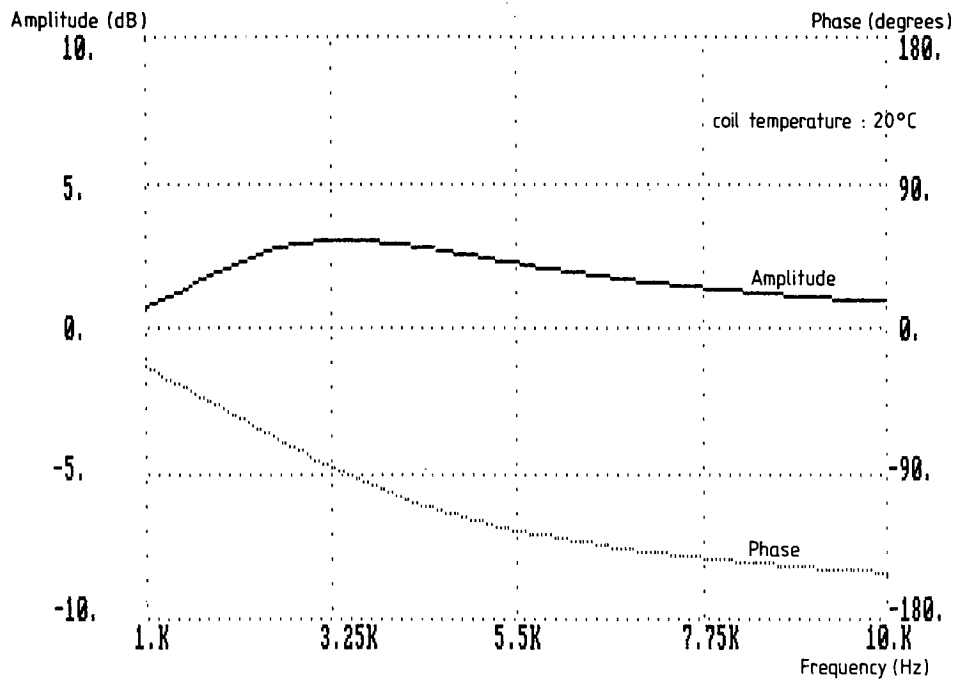
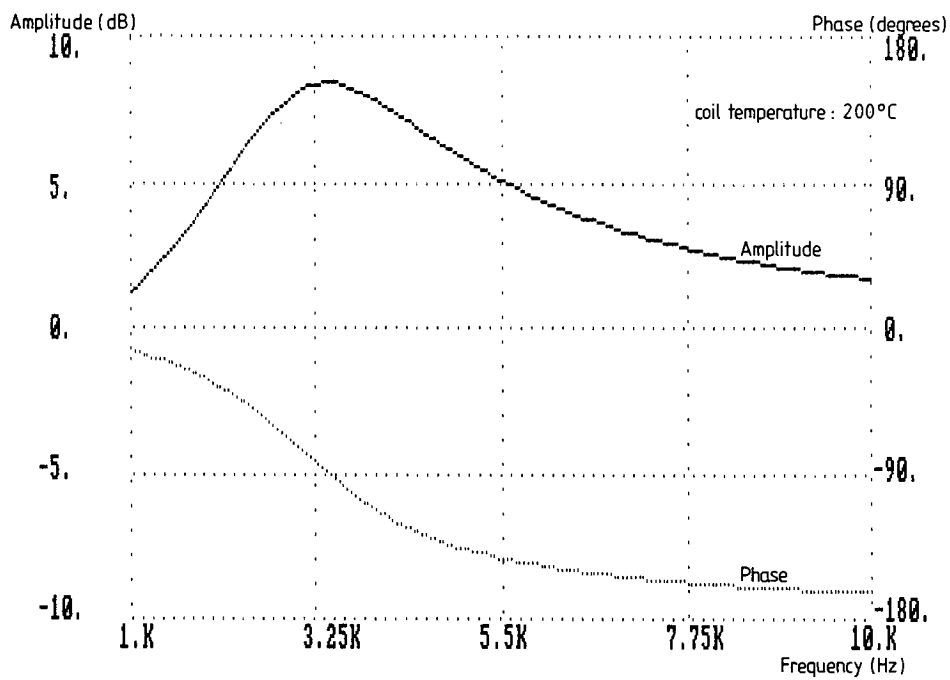


Fig. 7. Idealized two-way system with second-order crossover.



(a)



(b)

Fig. 8. Summed high-pass and low-pass outputs for idealized two-way system. (a) at 20°C. (b) at 200°C.

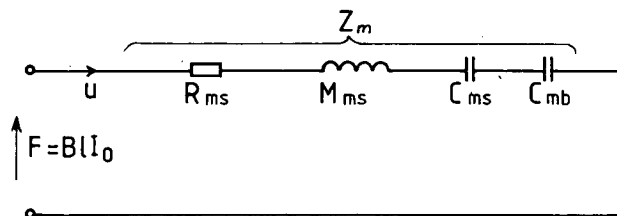


Fig. 9. Mechanical model of drive unit in sealed enclosure under current drive.

that is,

$$X(s) = \frac{s^2 T_c^2 + s T_c^2 / T_s Q_m + T_c^2 / T_s^2}{s^2 T_c^2 + s T_c / Q_c + 1} \quad (3)$$

The equalizer used for experimental purposes is represented by the cascaded integrator structure of Fig. 15. Comparing the transfer function of this system with $X(s)$ in Eq. (3), the time constants, are

$$T_1 = Q_c T_c$$

$$T_2 = \frac{T_c}{Q_c}$$

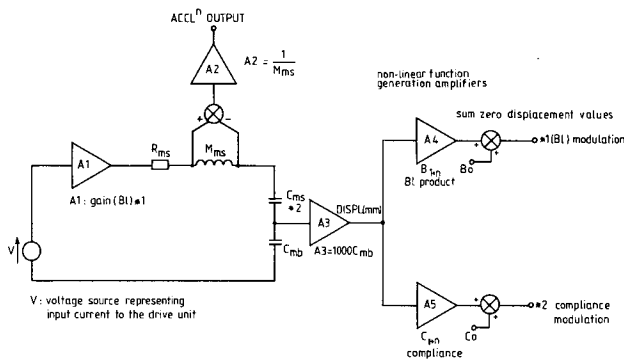


Fig. 10. Simplified nonlinear model for current-driven simulation.

and the summing constants,

$$C_1 = 1$$

$$C_2 = \frac{Q_c T_c}{Q_m T_s}$$

$$C_3 = \frac{T_c^2}{T_s^2}$$

This gives the ability to redefine the system Q and, if required, provide low-frequency extension.

Computer simulation of the equalizer and the example drive-unit-enclosure combination shows in Fig. 16(a) the overall system response for a Q realignment to 0.7071 with no resonant frequency shift, while Fig. 16(b) shows the effect of a resonance realignment to 40 Hz, with $Q = 0.7071$.

The disadvantage of this approach is the sensitivity to drive-unit mechanical parameter changes. To investigate this effect, the drive-unit mechanical parameters were subjected to $\pm 20\%$ tolerance and a Monte Carlo analysis based on 25 trials carried out to show the effect of random parametric variations within this range. The results reveal a 2-dB response error standard deviation around the area of fundamental resonance in both cases. However, in practice, mechanical parameter variations are likely to be better controlled with a well-engineered drive unit.

A novel technique of altering low-frequency realignment, which has been described in [22], is the "ace bass" system after Stahl. This method relies on

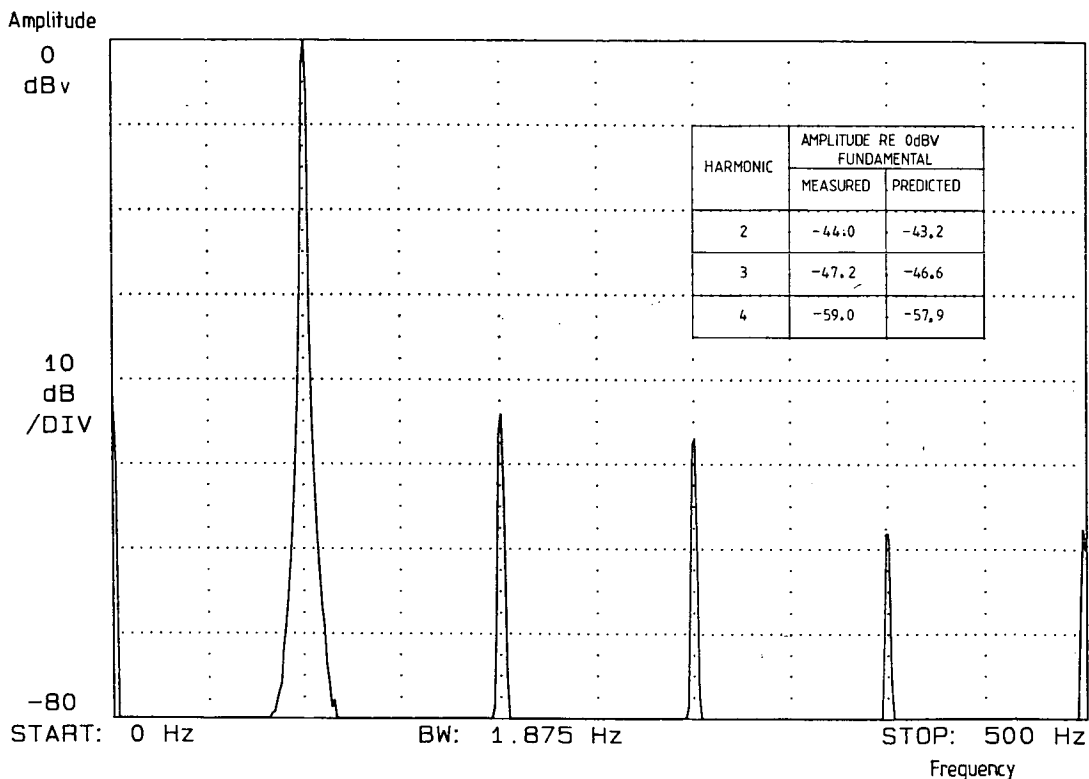


Fig. 11. Measured 100-Hz harmonic distortion, current driven. Table compares with predicted result.

providing the power amplifier with both a negative output resistance to cancel the drive-unit resistance and a synthesized parallel reactance in effect to modify the drive-unit mechanical parameters. While this technique does exhibit insensitivity to mechanical parameter variations (less than 1-dB standard deviation error on

the same basis as the open-loop compensator for 40-Hz realignment), it does, as the author admits, incur problems due to voice-coil heating. The error for our example drive unit is shown in Fig. 17, by computer simulation with the voice-coil temperature at 20°C (reference) and increased to 200°C, where the low-

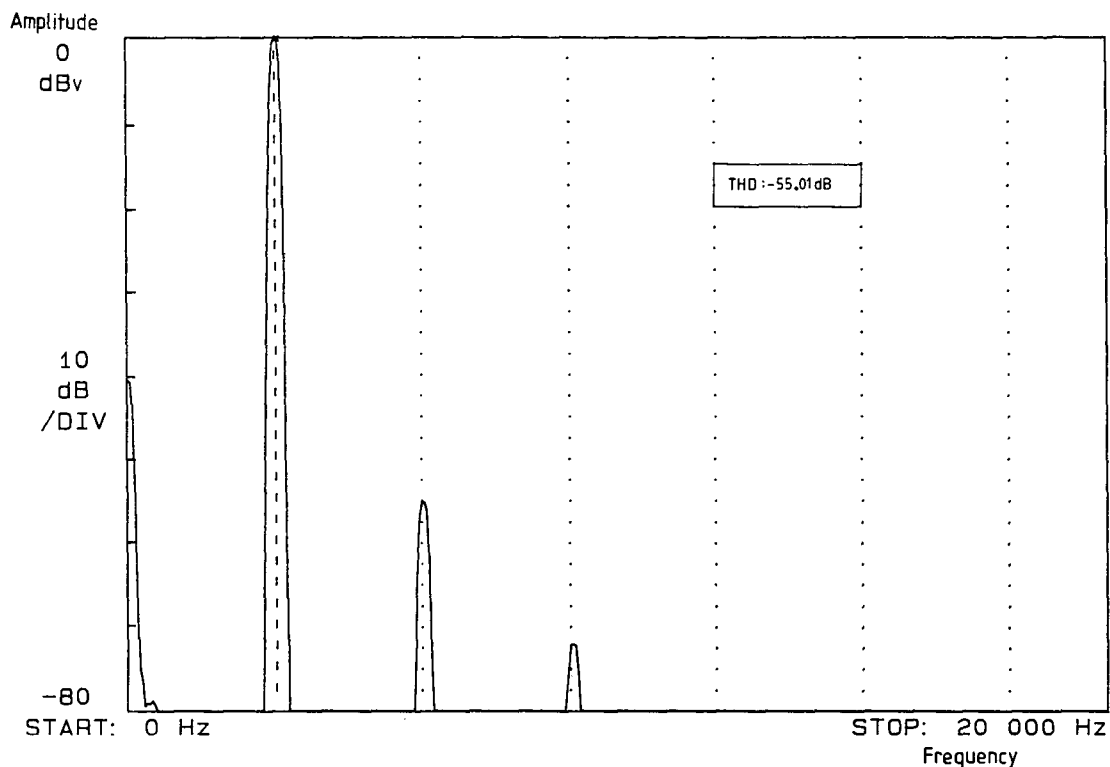


Fig. 12. Measured 3-kHz harmonic distortion, current drive.

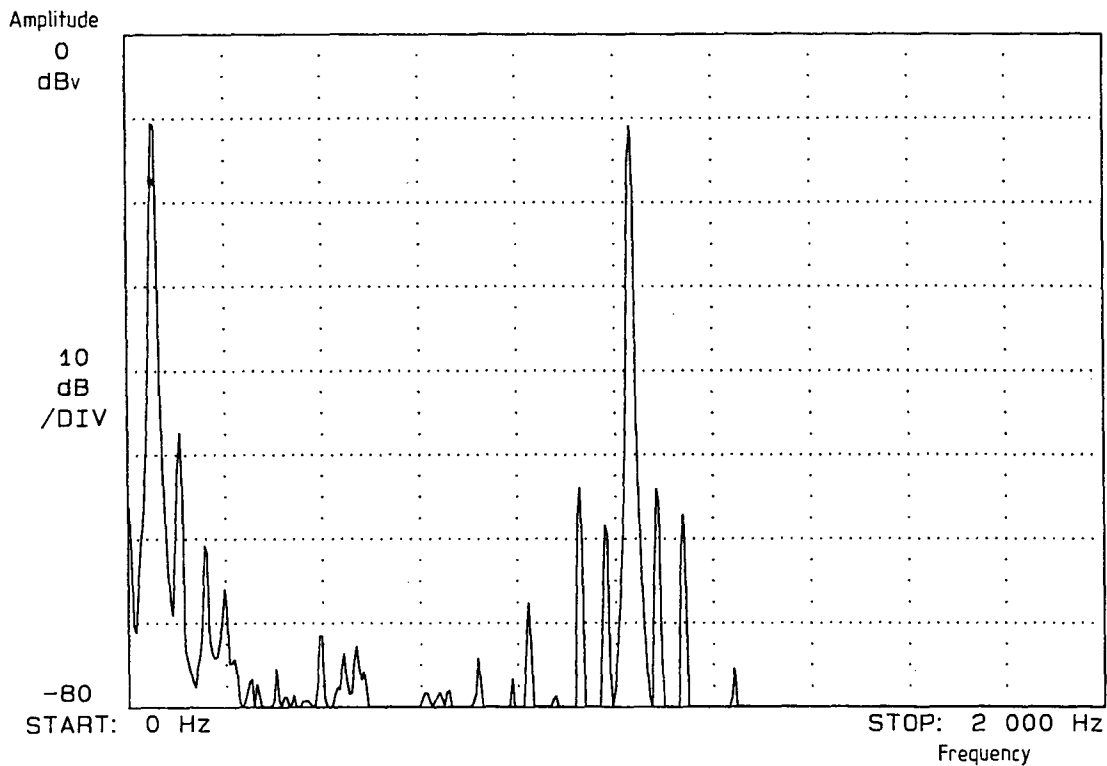
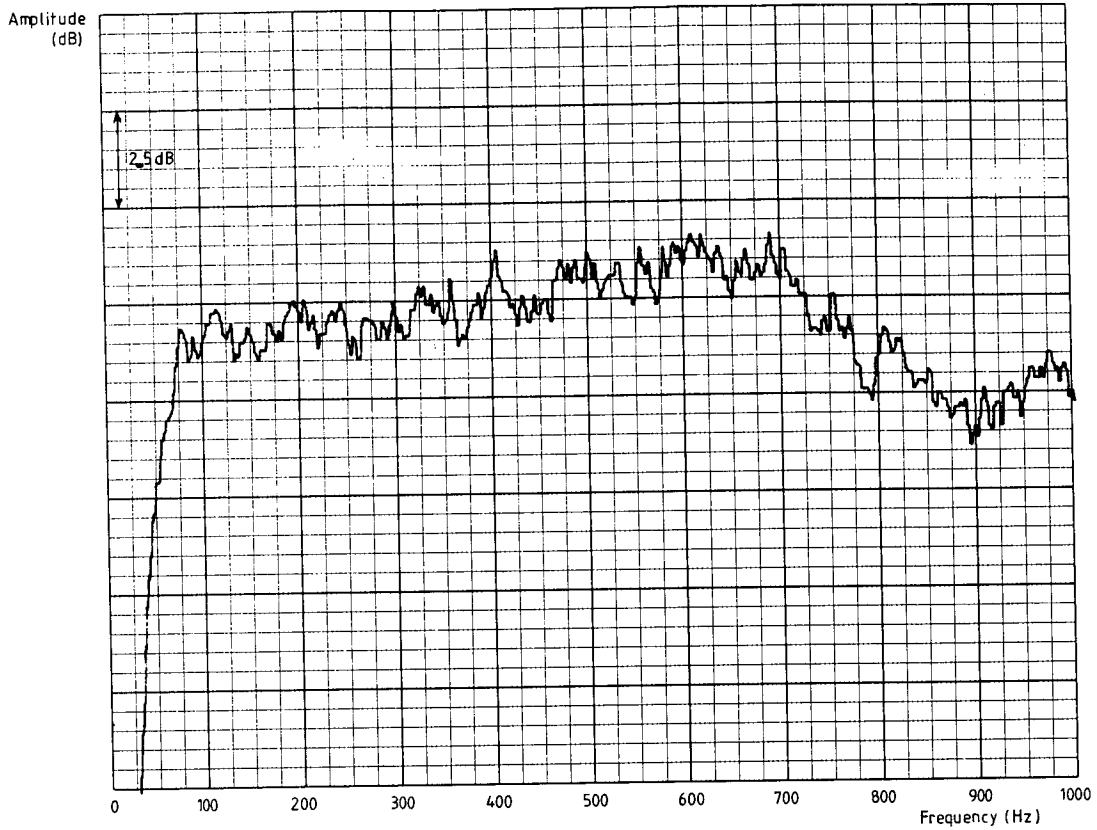
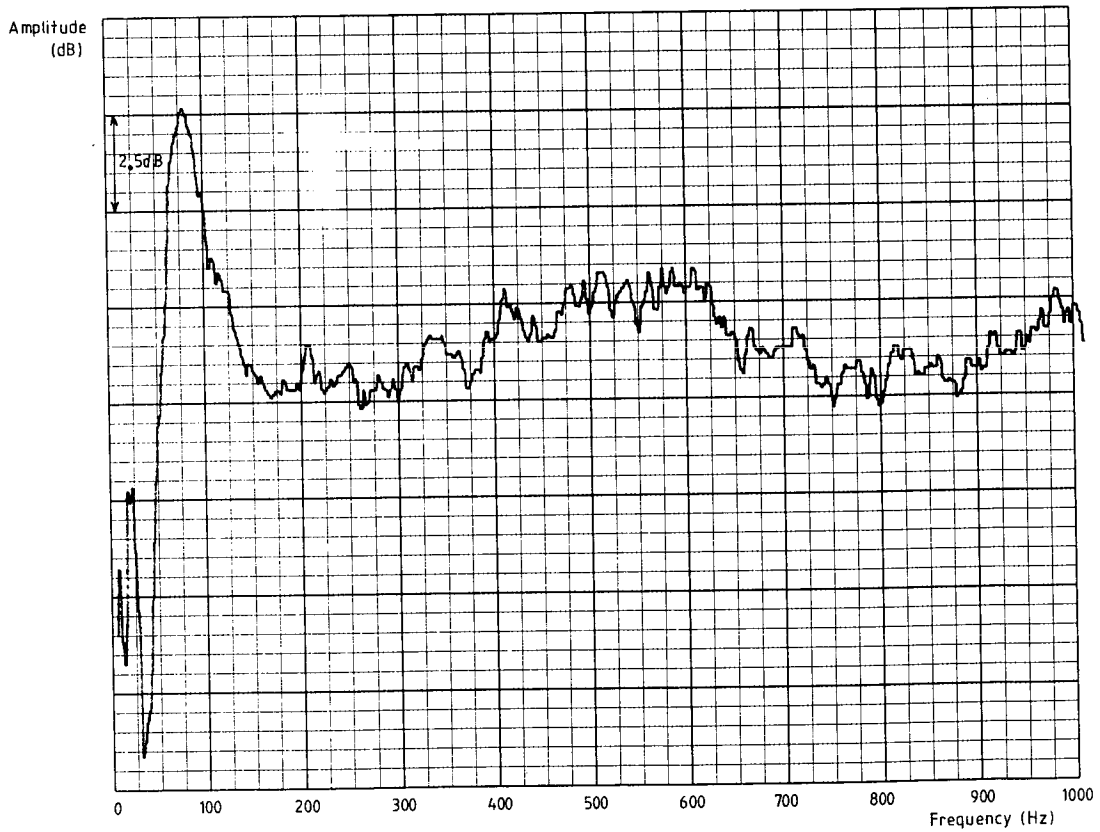


Fig. 13. Measured 50-Hz and 1-kHz intermodulation distortion, current driven.



(a)



(b)

Fig. 14. Measured frequency response of example drive unit. (a) Voltage drive. (b) Current drive.

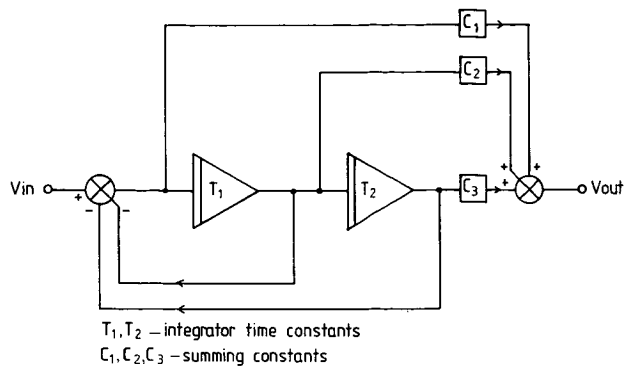


Fig. 15. Representation of open-loop equalizer.

frequency alignment was set to 40-Hz resonance with $Q = 0.7071$. Where low-frequency extension is required, the extra power needed to combat the drive unit's falling response means that coil heating effects are particularly troublesome, hence reinforcing the need for current drive in this type of application.

3.2 Motional Feedback

Motional feedback is considered the optimal method for Q alignment of low-frequency drive units under current control and was consequently incorporated into the prototype development system. Our earliest reference to the technique is due to Voight in 1924 [23],

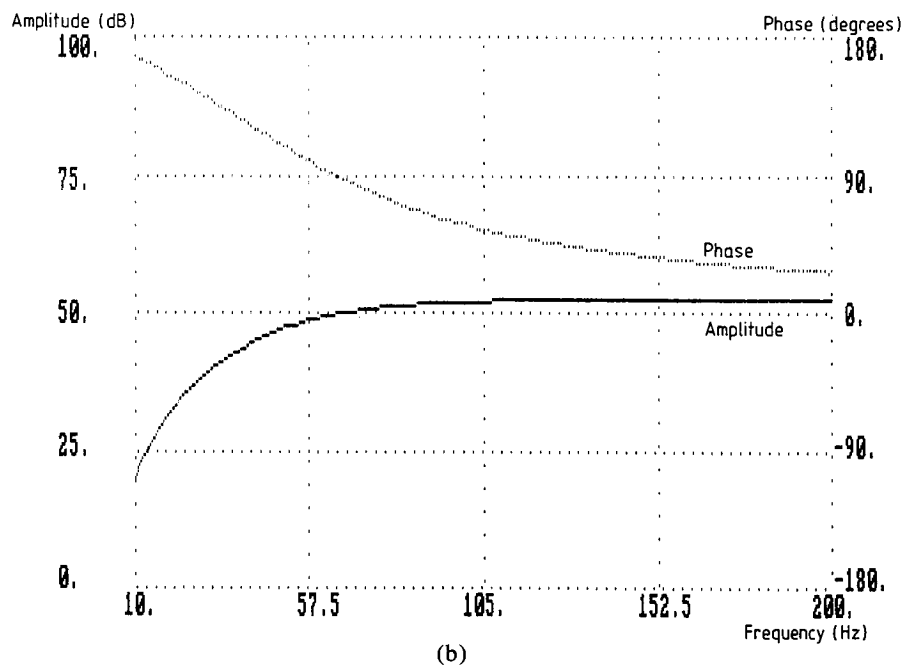
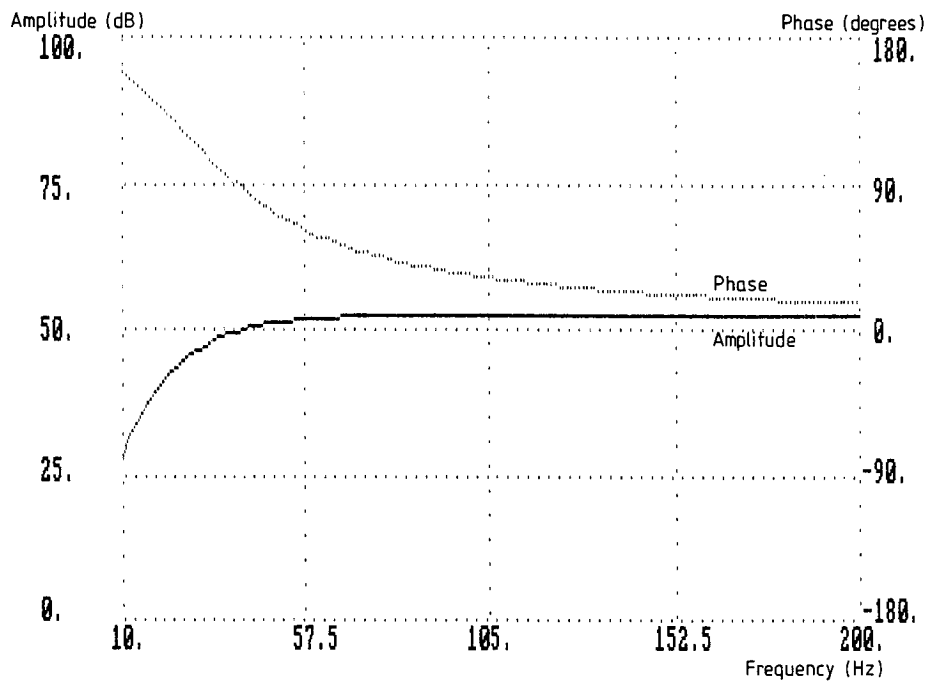


Fig. 16. Simulated current-driven system response with equalizer. (a) No resonance change (65 Hz), $Q = 0.7071$. (b) Resonance lowered to 40 Hz, $Q = 0.7071$.

where the lack in damping from an open-loop tube output stage led to similar problems as faced under pure current drive. The approach was later abandoned for general use when Black [24] formalized negative feedback techniques and amplifier output impedance could be reduced. Since then there has been much interest in motional feedback in high-performance applications, using a variety of sensing methods to obtain velocity, displacement, or acceleration feedback [25]–[28].

The method selected in this study was to wind a

sensing coil over the primary drive coil for reasons of cost effectiveness, with little additional complexity over a standard drive unit. The penalty of this mechanical simplicity is that as well as generating a signal proportional to cone velocity, there is also transformer coupling that induces an error from the driving coil into the sensing coil. Methods used to deal with this effect have included the use of additional neutralizing coils [29], [30]. In this case, the rather different method of electronic compensation has been adopted. Fig. 18 shows how this has been achieved, together with a

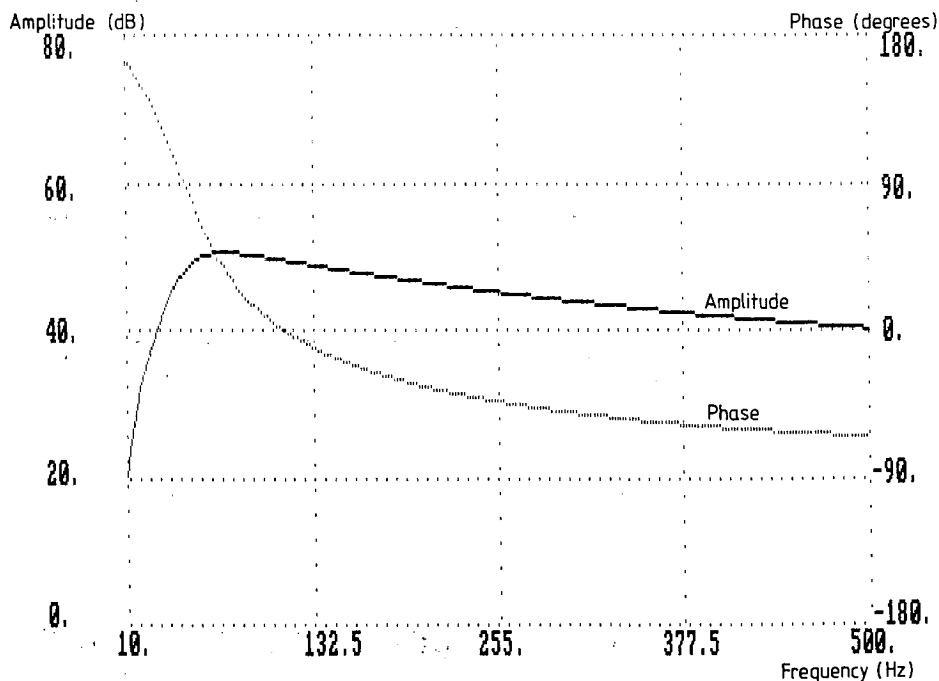
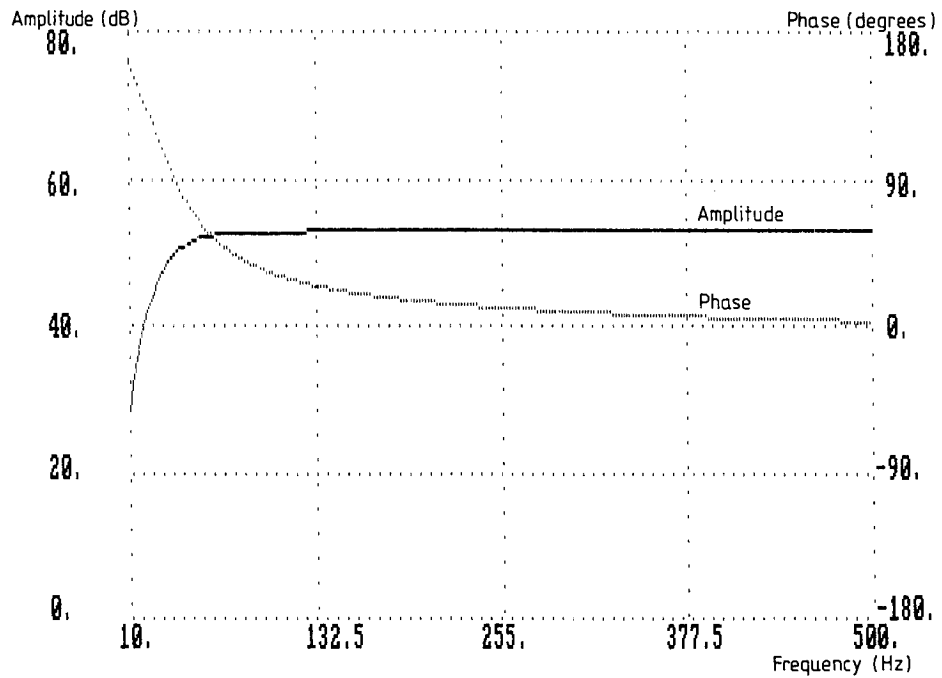


Fig. 17. “Ace bass” system frequency response simulations. Resonance set to 40 Hz, $Q = 0.7071$. (a) Voice-coil temperature 20°C. (b) Voice-coil temperature 200°C.

block diagram of the prototype system. So that the sensing coil does not reintroduce thermal errors, it must be interfaced to a high-input impedance buffer amplifier. The coupling error compensator consists of a filter matched to the transfer function of the coupling error characteristic, which increases by around 15 dB per decade up to 1 kHz at zero coil displacement. Some change in both the magnitude and the slope of this error is apparent with coil displacement, together with an unpredictable response above 1 kHz. To reduce this high-frequency residual error, the second-order low-pass filter at 1 kHz in the velocity feedback loop proves effective and in any event is required to maintain loop stability. Measurements have shown no increase in high-frequency distortion (at 3 kHz) over the open-loop case, indicating the effectiveness of this method.

To analyze the system, consider the simplified representation of Fig. 19, consisting of transconductance power amplifier, drive unit with sensing coil, and feedback path. The output voltage from the sensing coil V_s is written

$$V_s = (Bl)_s u$$

where $(Bl)_s$ is the sensing coil Bl product, in newtons per ampere, and u is the cone velocity, in meters per second. Also,

$$I_0 = [V_{in} - k(Bl)_s u] g_m$$

where

- I_0 = amplifier output current, amperes
- V_{in} = input voltage, volts
- k = feedback constant
- g_m = amplifier transconductance, siemens.

Using Eq. (2),

$$u = (Bl) [V_{in} - k(Bl)_s u] Y_m g_m$$

where Y_m is the admittance of the mechanical drive-unit model of Fig. 9. Thus

$$u = \frac{V_{in} (Bl) g_m}{1/Y_m + k(Bl)_s (Bl) g_m} \quad (4)$$

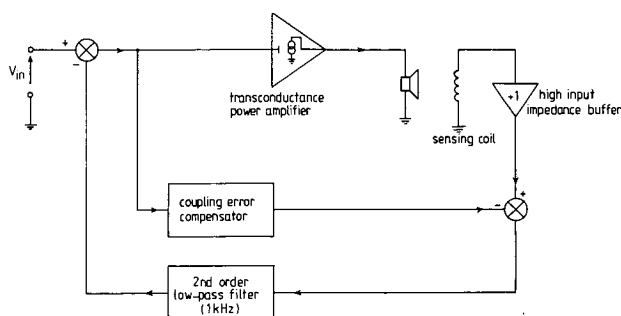


Fig. 18. Block diagram of prototype motional feedback system.

Examining the mechanical drive-unit model reveals

$$Y_m = \frac{sC_{mt}}{s^2 M_{ms} C_{mt} + sC_{mt} R_{ms} + 1} \quad (5)$$

where C_{mt} is the total mechanical compliance of the system, that is,

$$C_{mt} = \frac{C_{ms} C_{mb}}{C_{ms} + C_{mb}}$$

Substituting this result into Eq. (4) gives

$$u = [V_{in} (Bl) s C_{mt} g_m] [M_{ms} C_{mt} \{s^2 + s(1/M_{ms}) [R_{ms} + (Bl)_s (Bl) k g_m] \omega_0 / Q + 1/M_{ms} C_{mt}\}^{-1}] \omega_0^2 \quad (6)$$

Thus, for a second-order system,

$$Q = \frac{1}{(C_{mt}/M_{ms})^{0.5} [R_{ms} + g_m k (Bl) (Bl)_s]} \quad (7)$$

which may be rearranged to give

$$k = \frac{1/Q (M_{ms}/C_{mt})^{0.5} - R_{ms}}{(Bl) (Bl)_s g_m} \quad (8)$$

Investigation of system performance was carried out as for the open-loop case, with nonlinear transient analysis followed by measurement. It should be noted that in the prototype, the sensing coil followed the same Bl profile as the main coil, although to achieve a further low-frequency distortion reduction over the open-loop case, a more elaborate linear sensing mechanism is required. The transient analysis model will not be detailed, as it follows the earlier methodology—the velocity feedback signal was derived from the voltage across the mechanical resistance R_{ms} , and the feedback path loop stability filter was set to 1 kHz, second order. No transformer coupling effects were included in the model. For a 100-Hz at 1A peak sine-wave excitation, the measured distortion spectra are shown in

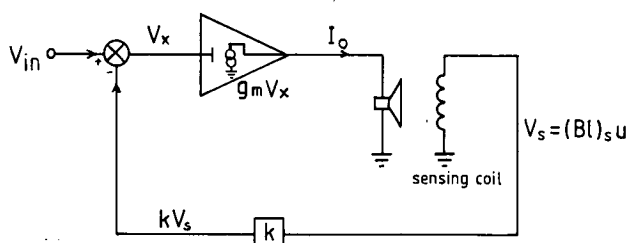


Fig. 19. Simplified motional feedback model for analysis purposes.

Fig. 20, along with comparative data from the simulation for a system Q of 0.7071. The results are seen to be broadly similar to the open-loop case for nonlinear Bl sensing, with a distortion reduction of around 4 dB on

the second and third harmonics resulting from predicted linear velocity sensing.

The measured frequency response (Fig. 21) is seen to be flatter than both the voltage-driven and the open-

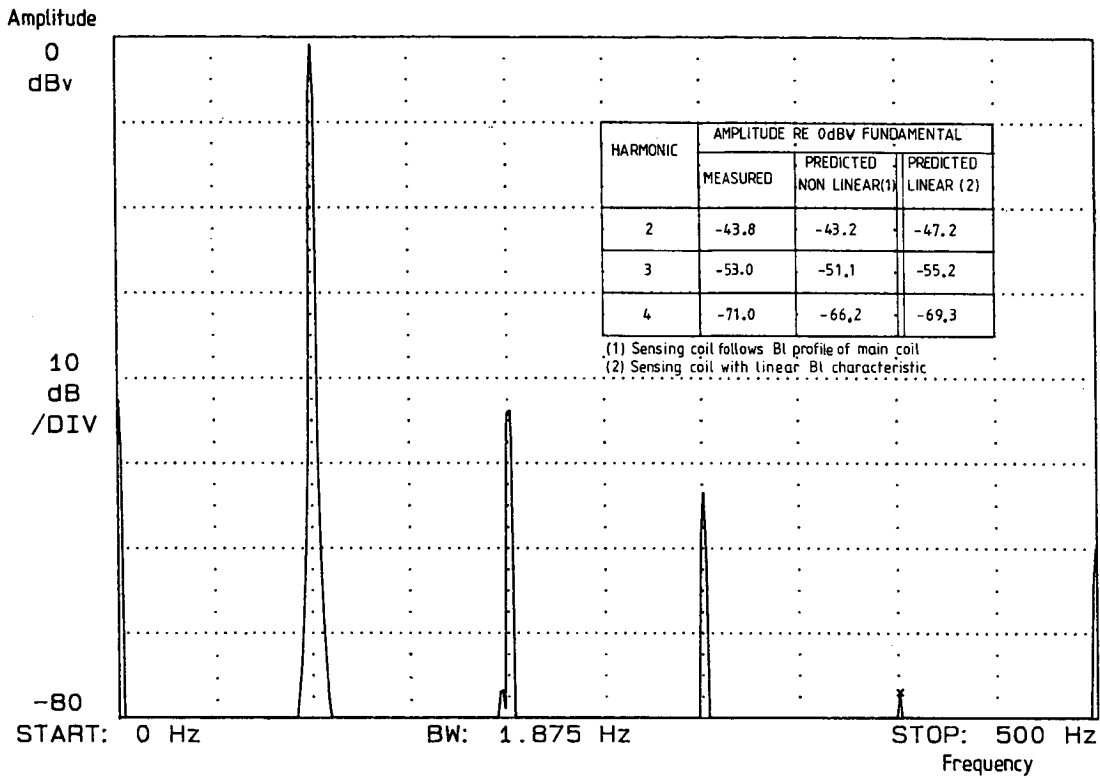


Fig. 20. Measured 100-Hz harmonic distortion, current driven with velocity feedback. Table compares with predicted results for both linear and nonlinear sensing-coil Bl profiles.

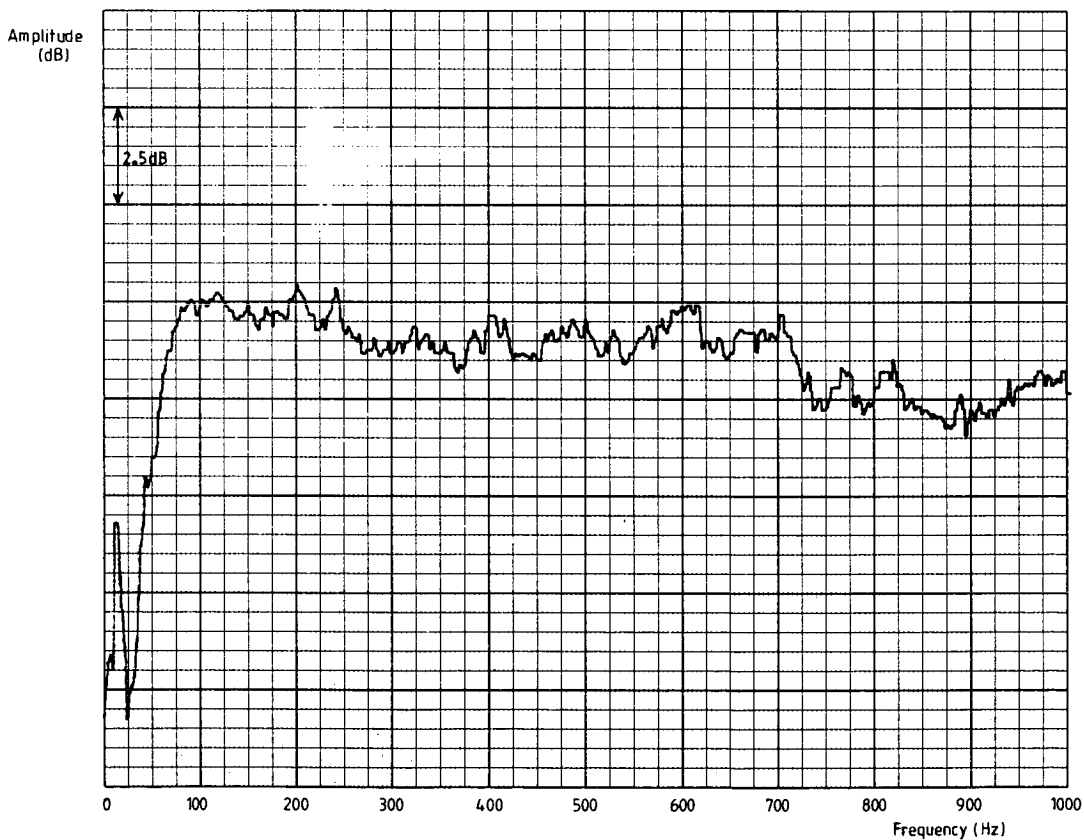


Fig. 21. Measured closed-loop frequency response for velocity feedback current-driven case, $Q = 0.7071$.

loop current-driven cases (Fig. 14). The effect of altering the feedback factor k is shown by the measured step responses in Fig. 22 for $Q = 3.0$ (open loop), $Q = 1.0$, and $Q = 0.7$.

3.3 High-Frequency Drive Unit with Electrically Conductive Former

At high frequencies, the preferred damping method is to use a drive unit with inherent electromagnetic damping through a conductive coil former. With such a device, experiment has shown a negligible contribution from voice-coil damping under voltage drive. Due to the improved linearity of high-frequency drive units, resulting from low coil displacement, the distortion reduction of current drive is less marked (around 3–7-dB reduction for drive units tested). However, the advantages in terms of freedom from thermally induced response errors and power compression are still valid.

4 POWER AMPLIFIER TOPOLOGIES FOR CURRENT DRIVE

A voltage-driven system requires a power amplifier with adequate bandwidth, low distortion, and a low output impedance which is linear and frequency independent. With current drive, the latter requirement translates to a high output impedance, which again should be linear and frequency independent. Also, the current demand under voltage drive [19], [31]–[34] becomes a problem of voltage demand under current drive. Consequently the maximum current delivery is known, which aids amplifier protection, as the system is inherently self-limiting.

The most basic strategy for generating a high output impedance is by the use of negative current feedback from a sensing resistor in the loudspeaker ground return [12], [13]. A typical configuration is shown in Fig. 23. Analysis of this system reveals that the transconductance g_m is given by

$$g_m = \frac{I_0}{V_{in}} = \frac{A}{(Z_0 + Z_L) + R_f(1 + A)} \quad (9)$$

where

- I_0 = load current, amperes
- V_{in} = input voltage, volts
- Z_0 = open-loop output impedance, ohms
- Z_L = drive-unit impedance, ohms
- R_f = current-sensing resistor, ohms
- A = forward gain of amplifier.

Consequently the output impedance Z_e may be written

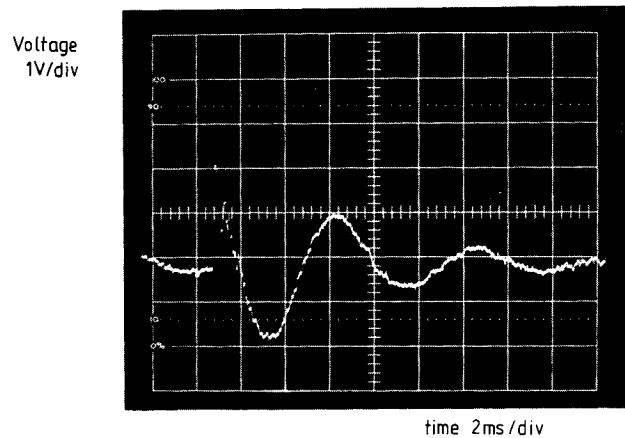
$$Z_e = (1 + A) R_f + Z_0 \quad (10)$$

This configuration, although a feasible solution, has two main limitations. First, the forward gain of the amplifier is frequency dependent, falling with increasing frequency as a result of its dominant pole. As a consequence, the output impedance falls with a similar

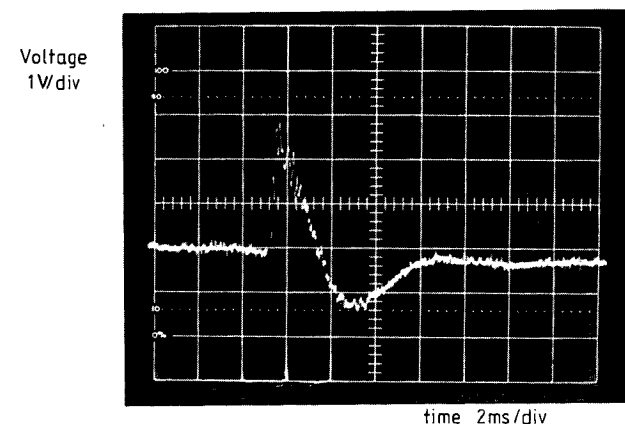
characteristic. Second, the loudspeaker impedance is both frequency dependent and nonlinear, leading to a modulation of the system transconductance [Eq. (9)] and being analogous to interface distortion in a conventional voltage amplifier.

To investigate this effect in more detail, consider an error function E_1 which is defined as

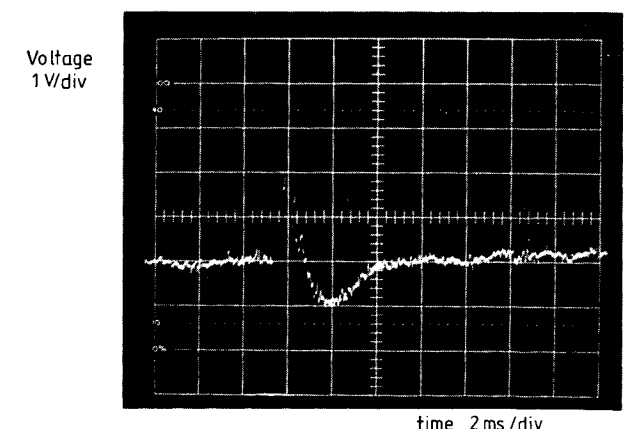
$$E_1 = \frac{g_m}{g_t} - 1$$



(a)



(b)



(c)

Fig. 22. Measured step responses for velocity feedback current-driven system. (a) $Q = 3.0$ (no feedback). (b) $Q = 1.0$. (c) $Q = 0.7$.

where g_t is the target transconductance, that is, $g_t = 1/R_f$. Thus, using Eq. (9),

$$E_1 = \frac{AR_f}{(Z_o + Z_L) + R_f(1 + A)} - 1$$

that is,

$$E_1 = - \frac{Z_o + R_f + Z_L}{(Z_o + Z_L) + R_f(1 + A)}$$

Assuming $(1 + A) R_f \gg (Z_o + Z_L)$,

$$E_1 \approx - \frac{Z_o + R_f + Z_L}{AR_f} \approx - \frac{Z_L}{AR_f} \tag{11}$$

If we suppose as a numerical example that E_1 should be less than 0.1%, then from Eq. (11),

$$A > \frac{1000Z_L}{R_f}$$

Hence, if R_f is set to 0.5Ω and Z_L assumes a maximum value of 20Ω , then $A_{dB} > 92$ dB. This is seen to be a high open-loop gain to maintain and illustrates well the limitations of the current feedback technique, particularly as Z_L is nonlinear.

A more optimal solution to the problem is to provide a cascaded open-loop grounded-base isolation stage in the amplifier structure to isolate the transconductance amplifier from the load, as shown in Fig. 24. Several advantages result from this enhanced technique.

- 1) Output impedance is essentially independent of the transconductance amplifier A_t , being a function of the grounded-base isolation stage.
- 2) Performance of amplifier A_t is isolated from the nonlinear load Z_L , thus eliminating interface distortion through loop gain modulation [see Eq. (11)].
- 3) Amplifier A_t can, if desired, operate in class A with its own supply $\pm V_{s1}$, which may be of low value to minimize power dissipation.

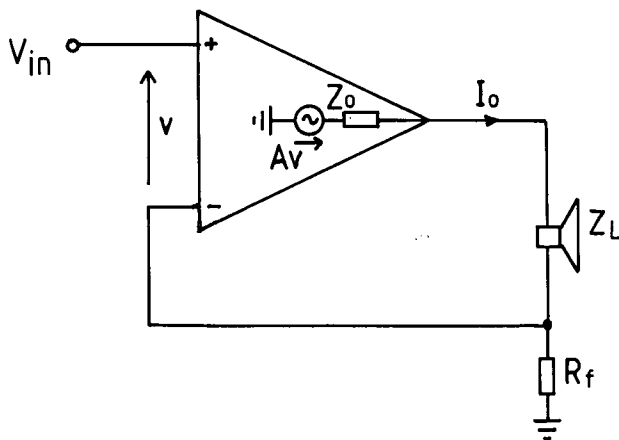


Fig. 23. Basic current feedback derived transconductance amplifier.

4) The grounded-base stage can operate in class AB, with a small standing current giving minimal distortion penalty, as current $I_L = I_0$, except for any base current leakage to ground.

5) Unlike the topology of Fig. 23, the loudspeaker load is referenced to ground, which simplifies installation and reduces the effect of interconnect capacitance at high frequencies.

6) If points P and Q (Fig. 24) are coincident, grounding-related errors are reduced due to signal currents forming well-defined closed paths.

7) The circuit topology is effectively a complementary cascode, therefore offering performance advantages in bandwidth and linearity.

8) As the grounded-base stage operates open loop, it does not degrade the loop gain and bandwidth characteristic of amplifier A_t .

9) The supply voltages $\pm V_{s2}$ can, in principle, be made adaptive to increase efficiency, when used in conjunction with a predictive digital processor.

Fig. 25 shows an alternative power amplifier topology, this time taking the form of a current gain stage. It must therefore be fed from a transconductance preamplifier. It has the advantage of having a ground-referenced power supply $\pm V_{s1}$ for the current amplifier A_i , meaning that in practice, several amplifiers in an active system may share a common supply, reducing complexity and cost.

Several prototype amplifiers have been built using these techniques. The first was based on the Fig. 24 complementary cascode configuration and operated with the transconductance amplifier A_t in class A with error feedback correction [35], [36], while the second was based on the Fig. 25 topology and used class AB operation for the current gain amplifier A_i with more extensive error correction and also moderate overall feedback. Both amplifiers were evaluated in terms of

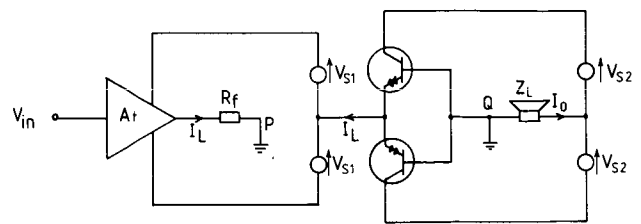


Fig. 24. Transconductance power amplifier using grounded-base output stage in complementary cascode configuration.

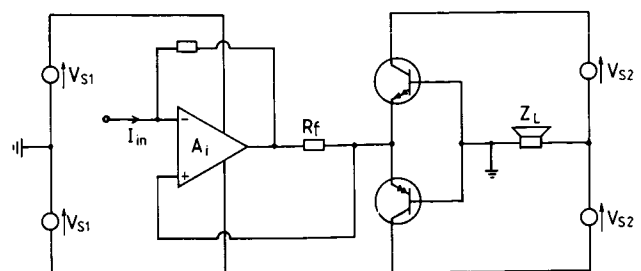


Fig. 25. Alternative power amplifier topology.

conventional measurements (Table 2) and were found comparable to typical high-performance voltage power amplifiers. On a practical note, it is judged important to provide adequate high-frequency current gain in the common-base stage to avoid distortion due to base leakage current to ground.

5 POWER AMPLIFIER AND DRIVE-UNIT PROTECTION UNDER CURRENT DRIVE

As the maximum available current from the transconductance power amplifier is an inherent design parameter, it is therefore self-limiting, so the system is simpler to protect. Indeed, this self-limiting characteristic implies that the designer need not be so concerned about protection circuitry, which has been cited as a source of degradation [37], [38].

Unlike the voltage power amplifier, which requires a series switching element for loudspeaker protection against offsets and other fault conditions, the current power amplifier requires a shunting element across the loudspeaker, thus avoiding the problems of contact degradation with time. Also a series fuse may be added without signal impairment, whereas with a voltage power amplifier, thermal modulation of the fuse wire resistance offers a source of distortion. Whereas a voltage amplifier requires short-circuit protection, a current amplifier is sensitive to open-circuit conditions. However, tests on the experimental amplifiers constructed have not given rise to a failure mode under open circuit.

A major factor concerning system reliability is drive-unit thermal failure. With conventionally powered loudspeakers, the coil current (and hence power dissipation) falls as temperature increases due to the thermal coefficient of the coil, giving a degree of protection. Elaborate protection systems have, however, been described for loudspeakers under voltage drive [39], [40]. Under current drive, no such self-limiting occurs. Indeed, it is an effect we are seeking to avoid. Thus, particularly for high-power and high-reliability installations, a method of sensing voice-coil temperature is required. This is best explained with reference to the block diagram system of Fig. 26. In addition to the main transconductance power amplifier and drive unit, a second low-power transconductance amplifier is provided to drive an impedance scaled model of the drive unit. In this model, R'_c represents the voice-coil resistance at room temperature and Z'_m the drive-unit motional impedance. After taking account of the scaling factors

in the current level and impedance of the reference network, the difference in voltage across the drive unit and reference network is obtained by a differential amplifier. The rms values of the input voltage V_{in} , which is proportional to the drive-unit current and of the differential amplifier output, are then fed to a divider network to produce a voltage V_{out} representing any increase in coil resistance due to heating. Presuming the temperature coefficient of the coil material is known, a measure of temperature is then determined.

The output voltage V_{out} may be used to drive a comparator to shut down power to the loudspeaker drive unit at a predetermined temperature. Alternatively, it can be used to progressively attenuate the drive-unit current to a safe level, or to provide curtailment of low-frequency extension to reduce power dissipation. The latter techniques are of particular interest to studio monitors, where high reliability and continuity of operation are paramount.

6 PROTOTYPE TWO-WAY ACTIVE LOUDSPEAKER SYSTEM

The ideas presented in this paper have been incorporated into a working prototype two-way active loud-

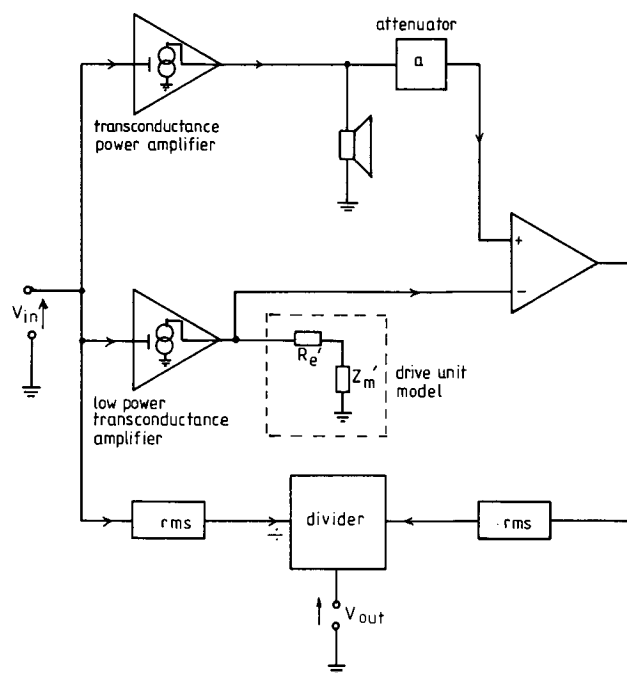


Fig. 26. Drive-unit thermal protection system for current drive.

Table 2. Performance comparison of prototype power amplifiers.

Measurement parameter	Test condition/notes	Class A design	Class AB design
Rated output power	8 Ω resistive load	75 W average	75 W average
Total harmonic distortion re rated power	20 Hz	-88 dB	-79 dB
	1 kHz	-84 dB	-86 dB
	20 kHz	-79 dB	-68 dB
Intermodulation distortion at rated power	19 kHz and 20 kHz at equal levels	< -90 dB	-86 dB
Hum and noise	Unweighted re full power	-91 dB	-90 dB
Small-signal bandwidth	-3 dB	dc-50 kHz	0.1 Hz-50 kHz

speaker system, based on the Celestion SL600 loudspeaker, because its high drive-unit quality and low level of enclosure coloration would theoretically make the benefits of current drive apparent on audition.

The system employs a discrete low-level electronic crossover, feeding individual current power amplifiers. One of the power amplifiers, based on the topology of Fig. 25, running in class AB with error correction is shown in detail in Fig. 27. Both power amplifiers are mounted on the loudspeaker stand, which aids thermal dissipation, with transformers mounted on the base to give mechanical stability. Fig. 28 shows the complete assembly. The crossover, motional feedback control circuits, coupling error compensator, and transconductance line amplifiers are housed in a separate enclosure (Fig. 29), which also incorporates level controls for the input signal. The crossover time constants are each independently adjustable for trimming, to enable comparison with the original voltage-driven loudspeaker to be made on a fair basis.

7 CONCLUSIONS

This paper has presented an alternative approach to the amplifier–loudspeaker interface, where numerous advantages have been cited through technical discussion, nonlinear computer modeling, and measurement. The principal advantages of current drive are seen to be an elimination of performance dependence on voice-coil resistance (which is thermally modulated) and also coil-inductive effects, which give rise to high-frequency distortion, along with nonlinear electromagnetic damping due to Bl variations. The technique is similarly insensitive to the lumped series elements of the amplifier–loudspeaker interconnect. However, it is often necessary to lower the system Q caused by the loss of amplifier-generated damping, either by open-loop compensation, by special drive-unit design, or by motional feedback, where the latter is regarded as the optimal method at low frequencies.

Having attempted a broad coverage of the principles of current drive, it is hoped that a greater interest in

and awareness of the technique will result. The authors perceive digital signal processing (DSP) as being integral to further developments in terms of crossovers, motion feedback signal processing, and drive-unit protection against thermal and excursion damage. The subject of digital crossover design has already been researched in depth within the Group. This resulted in a two-way working system, operating on the data stream from a CD player [41]. A further area of DSP to be investigated is compensation for the drive-unit Bl profile with coil displacement sensing, which under voltage drive would not be so amenable to correction, due to the more complicated nature of nonlinearities present in the system transfer function. In addition, DSP techniques have the potential to improve transconductance power amplifier efficiency by using modulated switched-mode power supplies.

While the research has been directed at moving-coil drive units, there is no reason why current drive should not be applied to ribbon transducers, which are often mechanically well damped and would benefit from removal of the matching transformer needed under voltage drive.

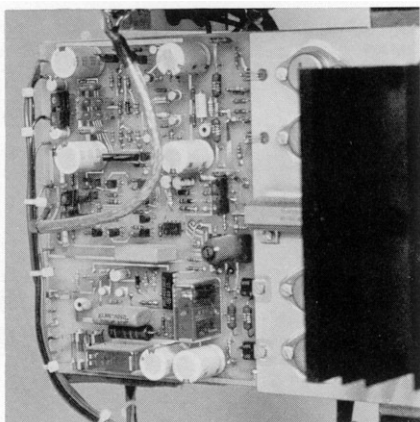


Fig. 27. View of prototype power amplifier based on Fig. 25.

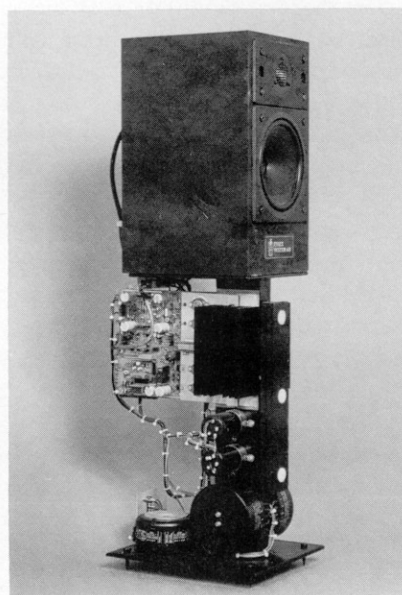


Fig. 28. Prototype active loudspeaker system.

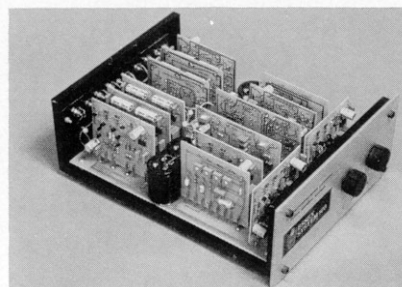


Fig. 29. View of control unit. System includes low-level crossovers, velocity feedback circuitry, and transconductance line amplifiers.

The technique of current drive should find wide applications in both high-performance domestic and studio applications, where it is felt that useful performance gains will be made over conventional systems.

8 ACKNOWLEDGMENT

This research was initially supported by the Science and Engineering Research Council of Great Britain under a research studentship program. Our thanks are due to Ed Form and more recently Graham Bank of Celestion International for providing the loudspeaker system used as the basis for the experimental work, along with the provision of modified drive units.

9 PATENT PROTECTION

The authors would like to point out that aspects of the work documented in this paper are the subject of a U.K. patent application.

10 REFERENCES

- [1] H. D. Harwood, "Loudspeaker Distortion Associated with Low-Frequency Signals," *J. Audio Eng. Soc.*, vol. 20, pp. 718–728 (1972 Nov.).
- [2] A. Dobrucki and C. Szmal, "Nonlinear Distortions of Woofers in the Fundamental Resonance Region," presented at the 80th Convention of the Audio Engineering Society, *J. Audio Eng. Soc. (Abstracts)*, vol. 34, p. 389 (1986 May), preprint 2344.
- [3] A. J. M. Kaizer, "Modeling of the Nonlinear Response of an Electrodynamical Loudspeaker by a Volterra Series Expansion," *J. Audio Eng. Soc.*, vol. 35, pp. 421–433 (1987 June).
- [4] R. J. Newman, "Do You Have a Sufficient Quantity of Acoustical Benzoin? Aspects Related to the Significance of Diaphragm Excursion," presented at the 80th Convention of the Audio Engineering Society, *J. Audio Eng. Soc. (Abstracts)*, vol. 34, p. 388 (1986 May), preprint 2342.
- [5] M. R. Gander, "Dynamic Linearity and Power Compression in Moving-Coil Loudspeakers," presented at the 76th Convention of the Audio Engineering Society, *J. Audio Eng. Soc. (Abstracts)*, vol. 32, pp. 1008–1009 (1984 Dec.), preprint 2128.
- [6] T. S. Hsu, S. H. Tang, and P. S. Hsu, "Electromagnetic Damping of High-Power Loudspeakers," presented at the 79th Convention of the Audio Engineering Society, *J. Audio Eng. Soc. (Abstracts)*, vol. 33, p. 1011 (1985 Dec.), preprint 2297.
- [7] C. A. Henricksen, "Heat-Transfer Mechanisms in Loudspeakers: Analysis, Measurement, and Design," *J. Audio Eng. Soc.*, vol. 35, pp. 778–791 (1987 Oct.).
- [8] W. J. Cunningham, "Nonlinear Distortion in Dynamic Loudspeakers due to Magnetic Effects," *J. Acoust. Soc. Am.*, vol. 21, pp. 202–207 (1949 May).
- [9] J. R. Gilliom, P. L. Boliver, and L. C. Boliver, "Design Problems of High-Level Cone Loudspeakers," *J. Audio Eng. Soc. (Project Notes/Engineering Briefs)*, vol. 25, pp. 294–299 (1977 May).
- [10] M. R. Gander, "Moving-Coil Loudspeaker Topology as an Indication of Linear Excursion Capability," *J. Audio Eng. Soc.*, vol. 29, pp. 10–26 (1981 Jan./Feb.).
- [11] H. F. Olson, "Analysis of the Effects of Non-linear Elements upon the Performance of a Back-Enclosed, Direct Radiator Loudspeaker Mechanism," *J. Audio Eng. Soc.*, vol. 10, pp. 156–163 (1962 Apr.).
- [12] J. A. M. Catrysse, "On the Design of Some Feedback Circuits for Loudspeakers," presented at the 73rd Convention of the Audio Engineering Society, *J. Audio Eng. Soc. (Abstracts)*, vol. 31, p. 364 (1983 May), preprint 1964.
- [13] R. A. Greiner and T. M. Sims, Jr., "Loudspeaker Distortion Reduction," *J. Audio Eng. Soc.*, vol. 32, pp. 956–963 (1984 Dec.).
- [14] M. J. Hawksford, "The Essex Echo—Unification," *Hi-Fi News Rec. Rev.*, pt. 1 (1986 May), pt. 2 (1986 Aug.), pt. 3 (1986 Oct.), pt. 4 (1987 Feb.).
- [15] M. N. T. Ojala and J. Lammasniemi, "Intermodulation Distortion at the Amplifier–Loudspeaker Interface," presented at the 59th Convention of the Audio Engineering Society, *J. Audio Eng. Soc. (Abstracts)*, vol. 26, p. 382 (1978 May), preprint 1336.
- [16] J. Lammasniemi and M. Ojala, "Power Amplifier Design Parameters and Intermodulation Distortion at the Amplifier–Loudspeaker Interface," presented at the 65th Convention of the Audio Engineering Society, *J. Audio Eng. Soc. (Abstracts)*, vol. 28, p. 380 (1980 May), preprint 1608.
- [17] R. R. Cordell, "Open-Loop Output Impedance and Interface Intermodulation Distortion in Audio Power Amplifiers," presented at the 64th Convention of the Audio Engineering Society, *J. Audio Eng. Soc. (Abstracts)*, vol. 27, p. 1022 (1979 Dec.), preprint 1537.
- [18] R. H. Small, "Direct-Radiator Loudspeaker System Analysis," *J. Audio Eng. Soc.*, vol. 20, pp. 383–395 (1972 June).
- [19] P. G. L. Mills and M. J. Hawksford, "Transient Analysis: A Design Tool in Loudspeaker Systems Engineering," presented at the 80th Convention of the Audio Engineering Society, *J. Audio Eng. Soc. (Abstracts)*, vol. 35, p. 386 (1986 May), preprint 2338.
- [20] S. H. Linkwitz, "Loudspeaker System Design," *Wireless World*, pp. 79–83 (1978 Dec.).
- [21] W. M. Leach, Jr., "Active Equalization of Closed-Box Loudspeaker Systems," *J. Audio Eng. Soc.*, vol. 29, pp. 405–407 (1981 June).
- [22] K. E. Stahl, "Synthesis of Loudspeaker Mechanical Parameters by Electrical Means: A New Method for Controlling Low-Frequency Loudspeaker Behavior," *J. Audio Eng. Soc.*, pp. 587–596 (1981 Sept.).
- [23] P. G. A. H. Voight, "Improvements in or Relating to Thermionic Amplifying Circuits for Telephony," UK Patent 231972 (1924 Jan.).
- [24] H. Black, "Inventing the Negative Feedback Amplifier," *IEEE Spectrum*, pp. 55–60 (1977 Dec.).

[25] J. A. Klaassen and S. H. de Koning, "Motional Feedback with Loudspeakers," *Philips Tech. Rev.*, vol. 29, no. 5, pp. 148–157 (1968).

[26] D. de Greef and J. Vandewege, "Acceleration Feedback Loudspeaker," *Wireless World*, pp. 32–36 (1981 Sept.).

[27] G. J. Adams, "Adaptive Control of Loudspeaker Frequency Response at Low Frequencies," presented at the 73rd Convention of the Audio Engineering Society, *J. Audio Eng. Soc. (Abstracts)*, vol. 31, p. 361 (1983 May), preprint 1983.

[28] E. de Boer, "Theory of Motional Feedback," *IRE Trans. Audio*, pp. 15–21 (1961 Jan./Feb.).

[29] A. F. Sykes, "Damping Electrically Operated Vibration Devices," UK Patent 272622 (1926 Mar.).

[30] R. L. Tanner, "Improving Loudspeaker Response with Motional Feedback," *Electronics*, pp. 142 ff. (1951 Mar.).

[31] I. Martikainen, A. Varla, and M. Ojala, "Input Current Requirements of High-Quality Loudspeaker Systems," presented at the 73rd Convention of the Audio Engineering Society, *J. Audio Eng. Soc. (Abstracts)*, vol. 31, p. 364 (1983 May), preprint 1987.

[32] D. Preis and J. Schroeter, "Peak Transient Current and Power into a Complex Impedance," presented at the 80th Convention of the Audio Engineering Society, *J. Audio Eng. Soc. (Abstracts)*, vol. 34, p. 386 (1986 May), preprint 2337.

[33] M. Ojala and P. Huttunen, "Peak Current Re-

quirement of Commercial Loudspeaker Systems," *J. Audio Eng. Soc.*, vol. 35, pp. 455–462 (1987 June).

[34] J. Vanderkooy and S. P. Lipshitz, "Computing Peak Currents into Loudspeakers," presented at the 81st Convention of the Audio Engineering Society, *J. Audio Eng. Soc. (Abstracts)*, vol. 34, pp. 1036–1037 (1986 Dec.), preprint 2411.

[35] M. J. Hawksford, "Distortion Correction in Audio Power Amplifiers," *J. Audio Eng. Soc.*, vol. 29 (*Engineering Reports*), pp. 27–30 (1981 Jan./Feb.).

[36] M. J. Hawksford, "Power Amplifier Output-Stage Design Incorporating Error-Feedback Correction with Current-Dumping Enhancement," presented at the 74th Convention of the Audio Engineering Society, *J. Audio Eng. Soc. (Abstracts)*, vol. 31, p. 960 (1983 Dec.), preprint 1993.

[37] T. Holman, "New Factors in Power Amplifier Design," *J. Audio Eng. Soc. (Engineering Reports)*, pp. 517–522 (1981 July/Aug.).

[38] M. Huber, "Important Aspects of Power Amplifiers," *Studio Sound*, pp. 66–74 (1985 Nov.).

[39] H. D. Harwood, "Improvements Relating to Loudspeakers," UK Patent 1520156 (1976 Mar.).

[40] D. R. von Recklinghausen, "Dynamic Equalizer System for Loudspeakers," UK Patent 2050754A (1980 Jan.).

[41] R. M. Bews, "Digital Crossover Networks for Active Loudspeaker Systems," Ph.D. dissertation, University of Essex, UK (1987 Sept.).

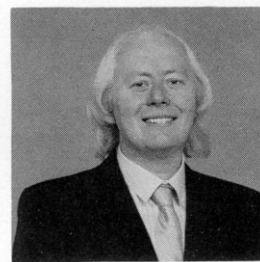
THE AUTHORS



P. Mills

Paul Mills graduated with a B.Eng. degree in engineering science and industrial management from Liverpool University in 1980. After working for GEC in power and control systems engineering, he began a 3-year period of postgraduate study at the University of Essex in 1983, during which time he formulated the ideas presented in this paper. He then taught at Essex for two years in the Electronics Systems Engineering Department, while writing his Ph.D. thesis on active loudspeaker systems with transconductance amplification. In 1988 July he was appointed senior design engineer with Tannoy Limited. He is a member of the Audio Engineering Society.

Malcolm Omar Hawksford is a senior lecturer in the Department of Electronic Systems Engineering at the University of Essex, where his principal interests are in the fields of electronic circuit design and audio engineering. Dr. Hawksford studied at the University of Aston in Birmingham and gained both a First Class



M. O. Hawksford

Honors B.Sc. and Ph.D. The Ph.D. program was supported by a BBC Research Scholarship, where the field of study was the application of delta modulation to color television and the development of a time compression/time multiplex system for combining luminance and chrominance signals.

Since his employment at Essex, he has established the Audio Research Group, where research on amplifier studies, digital signal processing, and loudspeaker systems has been undertaken. Since 1982 research into digital crossover systems has begun within the group and, more recently, oversampling and noise shaping investigated as a means of analog-to-digital/digital-to-analog conversion. Dr. Hawksford has had several AES publications that include topics on error correction in amplifiers and oversampling techniques. His supplementary activities include writing articles for *Hi-Fi News* and designing commercial audio equipment. He is a member of the IEE, a chartered engineer, a fellow of the AES, and a member of the review board of the *Journal*. He is also a technical adviser for *HFN* and *RR*.